VOLUME 122, NUMBER 26
JULY 5, 2000

JOURNAL OF THE AMERICAN CHEMICAL SOCIETY

Dendrimers Functionalized with a Single Fluorescent Dansyl Group Attached "Off Center": Synthesis and Photophysical Studies

Claudia M. Cardona,[†] Julio Alvarez,[†] Angel E. Kaifer,*[,†] Tracy Donovan McCarley,[‡] Siddharth Pandey,[§] Gary A. Baker,[§] Neil J. Bonzagni,[§] and Frank V. Bright*[,§]

Contribution from the Center for Supramolecular Science and Department of Chemistry, University of Miami, Coral Gables, Florida 33124-0431, Choppin Laboratories of Chemistry, Louisiana State University, Baton Rouge, Louisiana 70803-1804, and Department of Chemistry, Natural Sciences Complex, University of Buffalo, State University of New York, Buffalo, New York 14260-3000

Received March 16, 2000

Abstract: A series of three new fluorescent dendrimers containing a single, focally located dansyl group and 3 (**1**), 9 (**2**), and 27 (**3**) carboxylic acid groups in their peripheries were synthesized and characterized. The photophysical properties of these dendrimers were investigated in aqueous solution. The host−guest interactions of the dendrimers through their dansyl subunits with β-cyclodextrin and polyclonal anti-dansyl antibodies were also investigated by various methods. Photophysical measurements on the dendrimers demonstrate that the dansyl residue is progressively shielded from the solvent as the dendrimer generation increases, resulting in marked changes in spectral features, fluorescence quantum yields, excited-state fluorescence lifetimes, radiative and nonradiative decay rates, and rotational reorientation times. The excited-state intensity decay kinetics for **1**−**3** are well described by a single exponential. Contrary to the popularly held belief that lower generation dendrimers are "floppy" species in solution, the molecular motions of **1**−**3** are described by a single rotational reorientation time. Access to the dansyl moiety is impeded with increasing dendrimer size as the dendrimer mass affords a significant degree of protection from binding by nonselective (β-cyclodextrin (β-CD)) and selective (anti-dansyl antibody) hosts for the dansyl residue. The equilibrium constant for β-CD binding of the dansyl residue in **1** is ∼2.5-fold lower than that for binding to dansylamine (DA). Dendrimers **2** and **3** do not associate with β-CD at all. Anti-dansyl antibodies can bind to the dansyl residue in dendrimers **1**−**3** with remarkably large binding affinities. The equilibrium constant for the antibody complex decreases systematically from 5.0×10^7 M^{-1} for DA to 1.5×10^6 M^{-1} for **3**.

Introduction

Dendrimer functionalization is a very active area of research in modern chemistry.[1] In this regard, functionalization of dendritic structures with luminescent groups has attracted considerable attention because the molecular architecture of these systems offers interesting possibilities concerning light harvesting, energy storage, and conversion.[2] As a recent example, Fréchet and co-workers have synthesized dendritic macromolecules containing multiple light-harvesting chromophores in their periphery that, upon photoexcitation, can

[†] University of Miami.
[‡] Louisiana State University.
[§] State University of New York.

(1) For recent reviews on dendrimer research, see: (a) Bosman, A. H.; Janssen, H. M.; Meijer, E. W. *Chem. Rev.* **1999**, *99*, 1665. (b) Newkome, G. R.; He, E.; Moorefield, C. N. *Chem. Rev.* **1999**, *99*, 1689. (c) Fischer, M.; Vögtle, F. *Angew. Chem., Int. Ed.* **1999**, *38*, 884.

10.1021/ja000949l CCC: $19.00
Published on Web 06/16/2000

transfer energy efficiently to a single central core.[3] The excited core, in turn, releases the excitation energy by fluorescing.

While synthetic progress with functionalized dendrimers continues at a fast pace, detailed physicochemical studies on their properties lag somewhat behind. In this work, we report the synthesis of a series of unsymmetric dendrimers (first, second, and third generations, see structures below) containing a single dansyl group[4] covalently attached "off center", that is, at a focal point in these macromolecules. Taking advantage of the well-known fluorescent properties of the dansyl group,[5] we have carried out a detailed photophysical investigation to ascertain the effect of the dendrimer structures on the microenvironment that surrounds the dansyl residues and on the dynamics of these macromolecular systems. We have also investigated the effects of the dendrimer structure on the binding interactions of the dansyl residue (guest) with β-cyclodextrin[6] (β-CD) and polyclonal anti-dansyl antibodies (hosts). All of these data are of considerable interest to improve our fundamental understanding of dendrimer properties. Furthermore, the structure of our dendrimers is well-suited to investigate *site isolation* properties in dendrimers and related macromolecules. The type of dendritic matrix used in this work, first developed by Newkome and co-workers,[7] has been less frequently investigated than the more commonly utilized Fréchet-type dendrimers.[3,8]

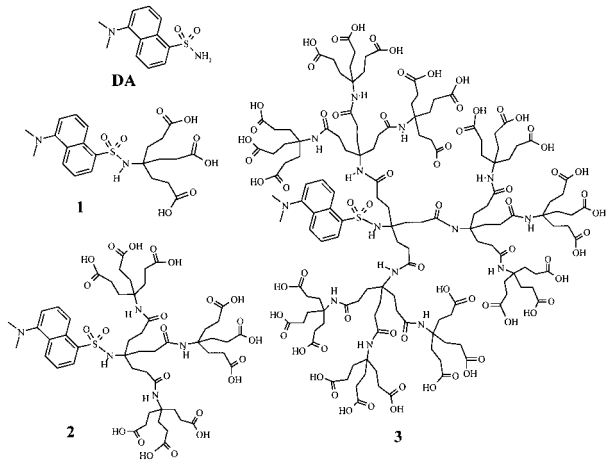

Results and Discussion

Synthesis. The synthetic procedures for the preparation of the dansyl dendrimers follow those previously reported by us for the synthesis of unsymmetric ferrocene-containing dendrimers.[9] Very briefly, dansyl chloride was reacted in dry acetonitrile with the corresponding amine building blocks to yield lipophilic forms of the dendrimers having *tert*-butyl groups on their periphery. Hydrolysis of these lipophilic dendrimers with formic acid leads to the more hydrophilic macromolecules **1**, **2**, and **3**, having 3, 9, and 27 surface carboxylic acid groups, respectively. This procedure is illustrated by the synthesis of dendrimer **2**, shown in Scheme 1. The overall dendrimer yields range from 44 to 67%. MALDI-TOF mass spectra were extremely important for the characterization of dendrimers **1**−**3**, providing verification of the purity of the precursor amine building blocks as well as of the completeness of the final hydrolysis process. We also prepared nitrotriacid **4** and nitrononaacid **5** for control experiments regarding cyclodextrin binding studies.

Scheme 1. Synthesis of Second Generation Dansyl Dendrimer **2**

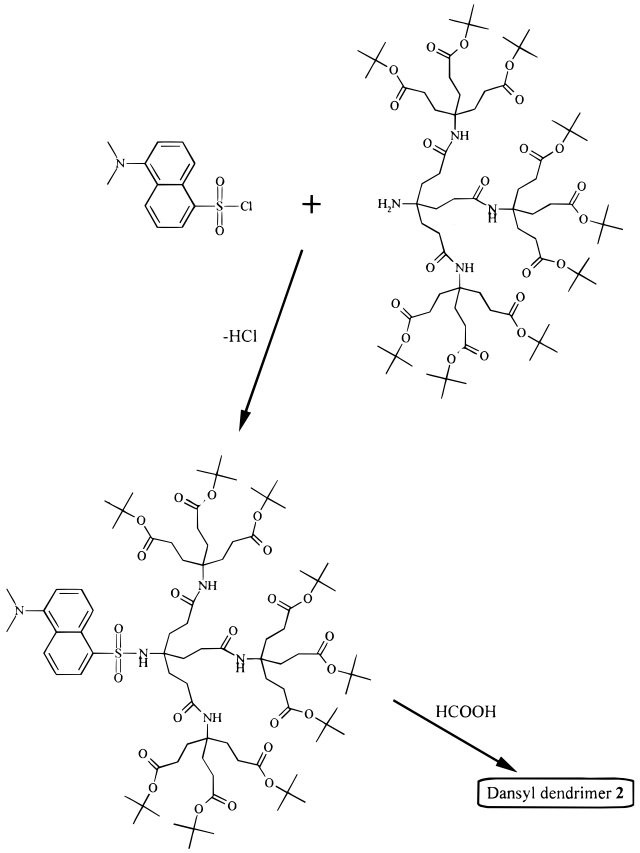

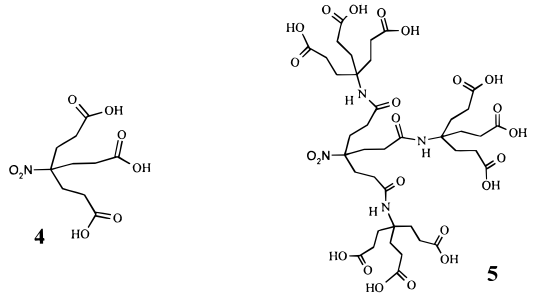

Steady-State Fluorescence Measurements. Absorbance and fluorescence maxima for dansylamide (DA) and dendrimers **1**−**3** (1 μM) dissolved in aqueous buffer are presented in Table 1. The hypsochromic shifts of the fluorescence spectra and the decrease in the Stokes shift suggest that the dansyl residue is systematically encountering a less polar microenvironment as the dendrimer generation increases from **1** to **2** to **3**. Although

(2) (a) Balzani, V.; Campagna, S.; Denti, G.; Juris, A.; Serroni, S.; Venturi, M. *Acc. Chem. Res.* **1998**, *31*, 26. (b) Jiang, D.-L.; Aida, T. *J. Am. Chem. Soc.* **1998**, *120*, 10895. (c) Devadoss, C.; Bharathi, P.; Moore, J. S. *J. Am. Chem. Soc.* **1996**, *118*, 9635.

(3) Adronov, A.; Gilat, S. L.; Fréchet, J. M. J.; Ohta, K.; Neuwahl, F. V. R.; Fleming, G. R. *J. Am. Chem. Soc.* **2000**, *122*, 1175.

(4) Multiple dansylation of poly(propylene imine) dendrimers has been recently reported: Archut, A.; Gestermann, S.; Hesse, R.; Kauffmann, C.; Vögtle, F. *Synlett* **1998**, 546.

(5) (a) Hoenes, G.; Hauser, M.; Pfleiderer, G. *Photochem. Photobiol.* **1986**, *43*, 133. (b) Li, Y.-H.; Chan, L.-M.; Tyer, L.; Moody, R. T.; Himel, C. M.; Hercules, D. M. *J. Am. Chem. Soc.* **1975**, *97*, 3118.

(6) For a series of recent reviews on the properties, uses and applications of cyclodextrin hosts, see: *Chem. Rev.* **1998**, *98*, 8, issue 5.

(7) Newkome, G. R.; Behera, R. K.; Moorefield, C. N.; Baker, G. R. *J. Org. Chem.* **1991**, *26*, 4376.

(8) Hawker, C. J.; Wooley, K. L.; Fréchet, J. M. J. *J. Am. Chem. Soc.* **1993**, *115*, 4375.

(9) Cardona, C. M.; McCarley, T. D.; Kaifer, A. E. *J. Org. Chem.* **2000**, *65*, 1857.

Table 1. Measured and Calculated Photophysical Parameters for Dansylamine (DA) and Dansyl-Labeled Dendrimers **1**, **2**, and **3** Dissolved in Aqueous Buffer (pH = 7)

solute	λ_{Abs}^{max} (nm)[a]	λ_{Flu}^{max} (nm)[b]	Φ_f	τ_f (ns)	k_r (10^7 s^{-1})	k_{nr} (10^8 s^{-1})	ϕ (ns)	V (nm^3)[c]
DA	324	548	0.028 ± 0.002	3.17 ± 0.02[d]	0.88 ± 0.06	3.07 ± 0.02	0.07 ± 0.01	0.29 ± 0.04
1	329	547	0.044 ± 0.003	4.90 ± 0.05	0.90 ± 0.06	1.95 ± 0.02	0.19 ± 0.02	0.77 ± 0.08
2	329	542	0.068 ± 0.003	6.32 ± 0.05	1.08 ± 0.05	1.47 ± 0.01	0.59 ± 0.03	2.40 ± 0.12
3	324	535	0.086 ± 0.003	7.94 ± 0.06	1.08 ± 0.04	1.15 ± 0.01	1.86 ± 0.05	7.57 ± 0.20

[a] Absorption maxima for repeat measurements are reproducible to within ±1 nm. [b] Fluorescence maxima have a ±2 nm imprecision. [c] Hydrodynamic volumes (V) are calculated from the Debye−Stokes−Einstein expression assuming viscosity η = 1 mPa·s at 22 °C. [d] The actual intensity decay for DA is best described by a double exponential decay law; the average value is reported here. The double exponential decay arises from the simultaneous emission from the locally excited and twisted intramolecular charge transfer states.

increasing the dendrimer generation might enhance the local polarity surrounding the dansyl residue because of the introduction of additional amide or carboxylate groups in proximity to the dansyl moiety, our data indicate that the enhanced hydrocarbon character predominates. Thus, an increase in dendrimer generation results in a less polar microenvironment surrounding the dansyl residue relative to DA dissolved in aqueous buffer.

Fluorescence Quantum Yields. The fluorescence quantum yields,Φ_f, of DA and **1**−**3** were determined (Table 1) by using the Parker and Rees method[10] with quinine sulfate dissolved in 0.1 N H_2SO_4 serving as the reference standard (Φ_s = 0.577). The results of this experiment show that the Φ_f value for the dansyl residue increases in the order DA < **1** < **2** < **3** and the increase parallels the hypsochromic shifts in the fluorescence spectra. It is important to mention here that the Φ_f value determined in this work for DA (0.028 ± 0.002) is statistically equivalent to the value reported for ϵ-dansyl-lysine (0.026−0.029) dissolved in water.[11] To provide the reader with a better feel for the increases in effective hydrophobicity surrounding the dansyl residue on going from DA to **3**, we note that **1** and **3** dissolved in aqueous buffer exhibit a Φ_f value similar to that measured for ϵ-dansyl-lysine dissolved in 90:10 and 80:20 (v:v) H_2O:dioxane mixtures, respectively.[11]

Excited-State Fluorescence Intensity Decay Kinetics. Figure 1 presents typical multifrequency phase-modulation[12−16] data sets for **1**−**3** dissolved in aqueous buffer. The symbols correspond to dendrimer **1** (■), **2** (▲), and **3** (●). The solid curves that pass through the data points are the best fits between the experimental data and a single-exponential decay law. In all cases, the time-resolved fluorescence intensity decay for **1**−**3** dissolved in buffer was well described by a single fluorescence lifetime, τ_f ($\chi^2 \leq 1.07$). Table 1 collects the recovered τ_f values. These results show that the fluorescence lifetime for the dansyl residue increases significantly as we proceed from DA to **3**.

Table 1 also collects the radiative, k_r, and nonradiative rates, k_{nr},[17,18] for DA and dendrimers **1**−**3** dissolved in aqueous buffer. These results show that the reason for the increase in τ_f on going from DA to **3** is a consequence of two factors: (1) a slight (∼20%) increase in k_r and (2) an almost 3-fold decrease in k_{nr}.

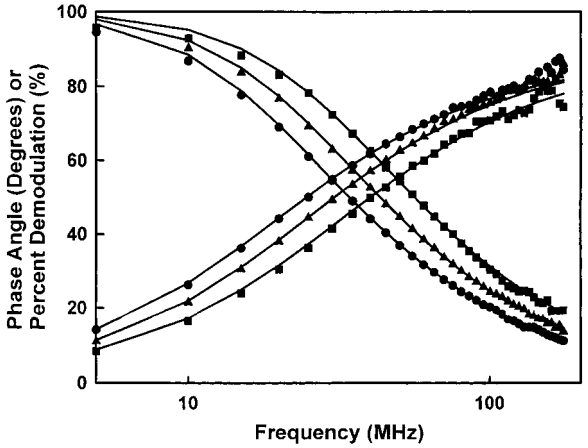

Figure 1. Typical multifrequency phase-modulation data for dendrimers **1** (■), **2** (▲), and **3** (●) dissolved in aqueous buffer (pH = 7.0). The solid curves represent the best fit between each data set and a single-exponential decay law.

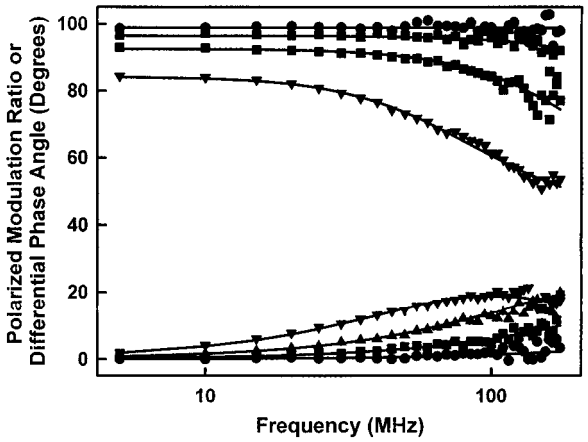

Figure 2. Typical multifrequency polarized modulation ratio and differential polarized phase angle data for DA (●), **1** (■), **2** (▲), and **3** (▼) dissolved in aqueous buffer (pH = 7.0). The solid curves represent the best fit between each data set and a isotropic rotor model with one rotational reorientation time.

These data indicate that successive dendrimer generations result in a shutting down of nonradiative pathways (e.g., twisted intramolecular charge transfer from the excited manifolds)[5] of the dansyl residue with very little change in radiative pathways.[17,18]

Figure 2 presents typical multifrequency polarized modulation ratio and differential polarized phase angle[12−16] data for DA and dendrimers **1**−**3** dissolved in aqueous buffer. The symbols correspond to DA (●) and dendrimers **1** (■), **2** (▲), and **3** (▼). The solid curves that pass through the data points are the best fits between the experimental data and an isotropic rotor model with a single rotational reorientation time, ϕ. In all cases, the time-resolved anisotropy decay for DA and **1**−**3** dissolved in

(10) Parker, C. A.; Rees, W. T. *Analyst* **1962**, *87*, 83.
(11) Parker, C. W.; Yoo, T. J.; Johnson, M. C.; Godt, S. M. *Biochemistry* **1967**, *6*, 3408.
(12) Lakowicz, J. R. *Principles of Fluorescence Spectroscopy*, 2nd ed.; Kluwer Academic/Plenum Publishers: New York, 1999.
(13) Bright, F. V.; Betts, T. A.; Litwiler, K. S. *Crit. Rev. Anal. Chem.* **1990**, *21*, 389.
(14) Gratton, E.; Jameson, D. M.; Hall, R. D. *Annu. Rev. Biophys. Biophys. Bioeng.* **1984**, *13*, 105.
(15) Jameson, D. M.; Gratton, E.; Hall, R. D. *Appl. Spectrosc. Rev.* **1984**, *20*, 55.
(16) Lakowicz, J. R.; Lackzo, G.; Gryczynski, I.; Szmacinski, H.; Wiczk, W. *J. Photochem. Photobiol. B: Biol.* **1988**, *2*, 295.
(17) Turro, N. J. *Modern Molecular Photochemistry*; University Science Books: Sausalito, CA, 1991.
(18) Birks, J. B. *Photophysics of Aromatic Molecules*; Wiley-Interscience: London, 1970.

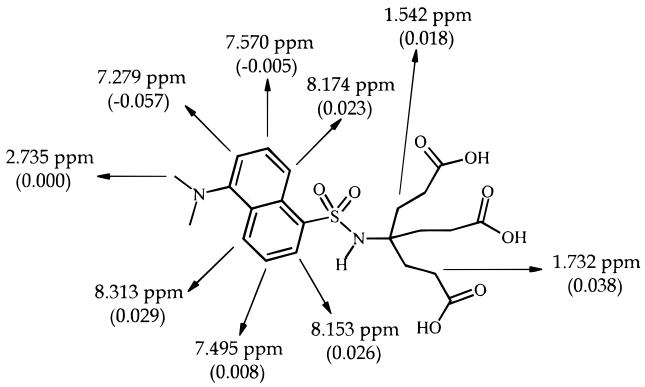

Figure 3. Chemical shift for the protons of **1** (1 mM) in D_2O buffered at pD 7.0. The values in parentheses indicate the shifts induced by the addition of 4 mM β-CD.

buffer was well-described by a single ϕ ($\chi^2 \leq 1.12$). Table 1 collects the recovered ϕ values. These results show that there is no evidence for the dansyl residue moving independently from the dendrimer; the dansyl unit moves in registry with the dendrimer's molecular framework.

The Debye−Stokes−Einstein expression[12] provides a convenient way to estimate the hydrodynamic volume, *V*, of the reorienting species. Table 1 collects the recovered *V* values for DA and **1**−**3**. Examination of Table 1 reveals that *V* increases systematically from DA to **1** to **2** to **3**.

Binding with Cyclodextrin Hosts. Dansyl derivatives are well-known guests for the formation of inclusion complexes with CD hosts.[19−21] Our interest in the investigation of host−guest interactions between these dansyl-containing dendrimers and cyclodextrins derives from previous results obtained with ferrocene-containing dendrimers.[9] Our electrochemical data suggested that the stepwise growth in the dendritic matrix (from first to second to third generation) effectively decreases the equilibrium association constant (K_a) between the dendrimer-attached ferrocene group and β-CD. This effect is presumably due to the increasing steric difficulty that the CD host encounters—as the dendritic matrix grows—to approach and engulf the ferrocene residue. In fact, cyclodextrin binding studies may constitute an additional method to probe how deeply buried is the functional group of choice into the dendritic matrix and provide insight into the extent of *environmental isolation* that the dendrimer affords to the guest unit (ferrocene, dansyl, etc.).

Initially we investigated binding of dendrimers **1** and **2** with β-CD using ^{1}H NMR spectroscopy. Figure 3 shows the changes in the observed chemical shifts for the proton resonances of dendrimer **1** induced by the addition of the β-CD host. Clearly, the aromatic protons in the dansyl unit, as well as the methylene protons in the three branches of the dendrimer unit, are sensitive to the presence of the CD. Regression analysis of the chemical shifts measured as a function of the concentration of added β-CD leads to a value of 110 M^{-1} for K_a. Similar experiments with dendrimer **2** yielded smaller β-CD-induced chemical shift changes (see Figure 4). Regression analysis of these data led to much smaller values of the corresponding K_a, but accurate values could not be determined with a reasonable confidence level because the binding is very weak. Notice that β-CD-induced chemical shifts in **2** were only observed for the protons of the first dendrimer layer, that is, the layer closer to the dansyl group. No interaction between the CD host and the outside, carboxylate-terminated layer of the dendrimer was detected from these NMR experiments. To further verify that the carboxylate surface of the dendrimer does not interact with β-CD, we performed NMR control experiments with dendrimers **4** and **5** in which the dansyl residue is replaced by a nitro group. Neither one of these compounds exhibited detectable β-CD-induced chemical shift changes, unequivocally confirming that the CD binding site in **1** and **2** is the dansyl residue. Our NMR data also indicate that the stability of the β-CD·**2** complex is much lower than that of the β-CD·**1** complex. We did not run similar NMR experiments with dendrimer **3** due to the well-documented problems encountered for the observation of core proton resonances in third and larger generation dendrimers.

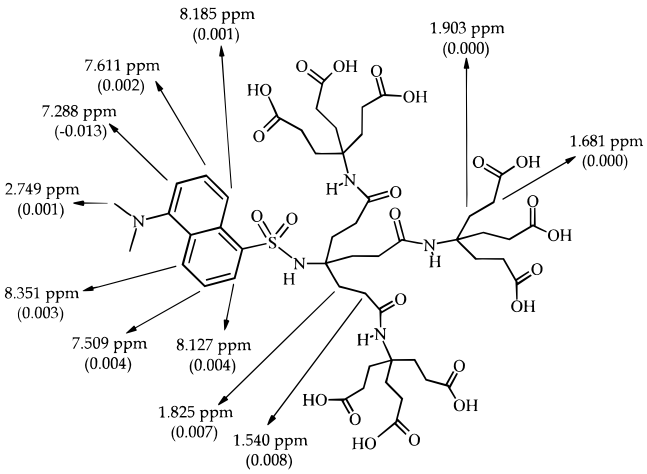

Figure 4. Chemical shift for the protons of **2** (1 mM) in D_2O buffered at pD 7.0. The values in parentheses indicate the shifts induced by the addition of 4 mM β-CD.

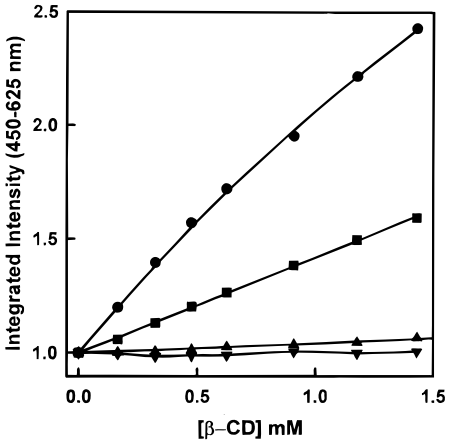

Figure 5. Effect of added β-CD on the steady-state fluorescence of for DA (●), **1** (■), **2** (▲), and **3** (▼) in aqueous buffer (pH = 7.0). The solid curves represent the regression analysis.

We also used steady-state fluorescence intensity and anisotropy methods[21] to determine the K_a values for binding of DA and **1**−**3** to β-CD. Figure 5 presents the integrated total dansyl fluorescence intensity as a function of added β-CD for DA (●) and dendrimers **1** (■), 2 (▲), and **3** (▼) dissolved in aqueous buffer. Examination of these data reveals that the addition of β-CD to the solution causes a marked increase in the dansyl group fluorescence intensity only for DA and **1**. The increase in fluorescence for **2** is nominal, and no statistical change in fluorescence intensity is observed for **3** upon addition of β-CD. According to these intensity profiles, dendrimer **3** is not bound by β-CD. To confirm the absence/presence of binding we measured the steady-state fluorescence anisotropy of DA and

(19) Dunbar, R. A.; Bright, F. A. *Supramol. Chem.* **1994**, *3*, 93.
(20) Ikeda, H.; Nakamura, M.; Ise, N.; Oguma, N.; Nakamura, A.; Ikeda, T.; Toda, F.; Ueno, A. *J. Am. Chem. Soc.* **1996**, *118*, 10980.
(21) Catena, G. C.; Bright, F. V. *Anal. Chem.* **1989**, *61*, 905.

Table 2. Recovered Equilibrium Association Constants, K_a, for Binding of DA and Dansyl-Labeled Dendrimers **1**, **2**, and **3** with β-CD in Aqueous Buffer (pH = 7.0) at 22 °C

complex	K_a (M^{-1})	r^2
DA + β-CD	307 ± 35	0.999
1 + β-CD	136 ± 23 110[a]	0.999
2 + β-CD	<1	0.957
3 + β-CD	~0 (no association observed)	

[a] from NMR measurements.

dendrimers **1**, **2**, and **3** as a function of added β-CD (data not shown). The anisotropy data confirm that **3** does not bind to β-CD, while association of **2** with β-CD is extremely weak. Table 2 collects the recovered K_a values for the complexation between DA and **1**−**3** with the β-CD host.

Inspection of the results presented in Table 2 shows several important points. The K_a recovered by fluorescence for **1** with β-CD is in good agreement with the value obtained using ^{1}H NMR spectroscopy (vide supra). However, although **1** can bind β-CD, its K_a is significantly lower than that for the β-CD·DA complex (307 vs 136 M^{-1}). Finally, the β-CD access to the dansyl residue in dendrimers **2** and **3** is totally impeded by the dendrimer mass.

Anti-Dansyl Antibody Binding. The binding between a hapten and an antibody can be a remarkably selective event that is often characterized by a high affinity ($K_a > 10^6$ M^{-1}). In contrast to other anti-fluorophore antibodies that quench the fluorescence of the fluorophore upon association, the association between polyclonal anti-dansyl antibodies and dansyl leads to a significant increase in the dansyl fluorescence and a hypsochromic spectral shift in the dansyl emission spectrum.[22,23] To assess the anti-dansyl/dendrimer K_a, we measured both the steady-state anisotropy and fluorescence intensity of the dansyl residue in DA and dendrimers **1**, **2**, and **3** as a function of added anti-dansyl antibody. This approach is superior to an intensity measurement alone because binding may not result in a measurable spectral shift and/or intensity change, but binding must be associated with a change in the steady-state fluorescence anisotropy and/or intensity.[21] Plots of steady-state fluorescence vs anti-dansyl concentration (not shown) indicated binding only for DA and **1** to anti-dansyl. While this is fully consistent with the β-CD results (Table 2), the intensity-based measurements are *not* conclusive evidence against binding between dendrimers **2** and **3** and anti-dansyl antibodies. [21]

Figure 6 presents the steady-state fluorescence anisotropy DA (●), **1** (■), **2** (▲), and **3** (▼) as a function of added antibody. These data clearly indicate that DA and dendrimers **1**, **2**, and **3** bind to polyclonal anti-dansyl antibodies. The recovered K_a values are compiled in Table 3. These results illustrate that: (1) there is remarkably strong binding between the dansyl residue within each dendrimer and the anti-dansyl antibody and (2) the K_a decreases only about 30-fold when we compare the binding affinity of DA (~5×10^7 M^{-1}) to that of dendrimer **3** (1.5×10^6 M^{-1}).

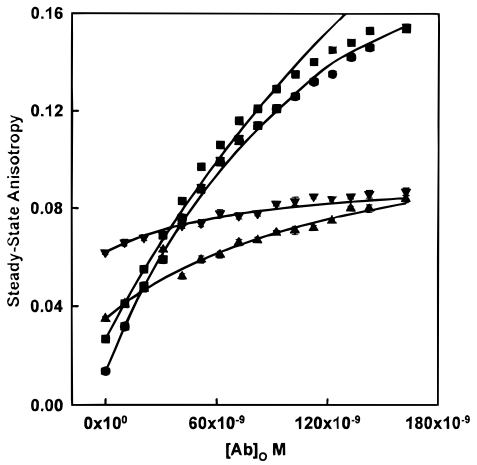

Figure 6. Effect of added anti-dansyl antibodies on the steady-state fluorescence anisotropy of for DA (●), **1** (■), **2** (▲), and **3** (▼) in aqueous buffer (pH = 7.0). The solid curves represent the regression analysis.

Table 3. Recovered Equilibrium Association Constants, K_a, for Binding of DA and Dansyl-Labeled Dendrimers **1**, **2**, and **3** with Polyclonal Anti-Dansyl Antibodies in Aqueous Buffer (pH = 7.0) at 22 °C

	from steady-state anisotropy		from fluorescence intensity	
complex	K_a (M^{-1})	r^2	K_a (M^{-1})	r^2
DA + Ab	$4.97 \pm 0.23 \times 10^7$	0.999	$1.40 \pm 0.51 \times 10^8$	0.987
1 + Ab	$4.07 \pm 0.20 \times 10^6$	0.997	$3.89 \pm 0.94 \times 10^6$	0.910
2 + Ab	$1.91 \pm 0.12 \times 10^6$	0.992	No association observed	
3 + Ab	$1.46 \pm 0.10 \times 10^6$	0.958	No association observed	

Conclusions

The results of these experiments illustrate several points. As the dendrimers grow, the dansyl residue encounters a significantly less polar microenvironment. The dansyl reporter group appears to move in concert with the entire dendrimer; no local motion was detectable. Association between a nonselective guest (β-CD) and the dansyl residue within the larger dendrimers can be impeded entirely. A selective host (anti-dansyl antibodies) can complex with each dendrimer to some degree, and the stability of the complexes was only decreased 30-fold when one compared the free guest to a sterically crowded dendrimer like **3**. This latter result is somewhat surprising given that β-CD and anti-dansyl differ by ~100-fold in mass (β-CD, 1135 g/mol; anti-dansyl, 150 000 g/mole), suggesting that the dendrimer conformation/structure can be altered to allow access to the dansyl residue if the binding affinity is great enough.

Experimental Section

Reagents for Synthesis. All chemicals were reagent grade (Aldrich) and were used as received. β-Cyclodextrin (β-CD) was a gift from Cerestar and used without any further purification. Solvents, such as CH_3CN, were freshly distilled. Column chromatography was performed with Scientific Adsorbents silica gel (63−200 μm).

3 Cascade:Dansyl[1]:(3-Oxo-2-azapropylidyne):Propanoic (1). Dansyl chloride (0.520 g, 1.93 mmol), Behera's amine (0.503 g, 1.21 mmol), and K_2CO_3 anhydrous (0.561 g, 4.01 mmol) were stirred in 10 mL of dry CH_3CN under N_2 at 23 °C. The progress of the reaction was followed by TLC (CH_2Cl_2). The reaction mixture was filtered, and the solvent was removed at reduced pressure. The residue was purified by column chromatography (SiO_2, CH_2Cl_2 followed by 5:1 CH_2Cl_2/EtOAc) to furnish the ester product (0.550 g, 70%) as a pale green foam. This compound was hydrolyzed by stirring the foam in 96% formic acid for 2 days to produce a white powder (95%) after complete removal of the formic acid under vacuum. FT-IR (KBr): 3300−2500 (ν(OH)) cm^{-1}; 3463 (ν(NH)) cm^{-1}; 1723 (ν(C═O)) cm^{-1}; 1569 (ν(AMIDE II, N−H)) cm^{-1}; 1317, 1142 (ν(S═O)) cm^{-1}. ^{1}H NMR (DMSO-d_6): 1.60−1.93 (m, CH_2CH_2, 12H); 2.81 (s, CH_3, 6H); 7.57

(22) Parker, C. W. In *Handbook of Experimental Immunology*; Weir, D. M., Ed.; Blackwell: Oxford, 1973; Vol. 1, Chapter 14.
(23) Hanson, D. C.; Yguerabide, J.; Schumaker, V. N. *Biochemistry* **1981**, *20*, 6842.

(sb, NH, 1H); 7.2−8.4 (m, $C_{10}H_6$, 6H); 12.0 (bs, OH, 3H). ^{13}C NMR (DMSO-d_6): 27.59, 30.33 (CH_2CH_2); 45.01 (CH_3); 60.45 ($C(CH_2CH_2)_3$); 114.85, 119.06, 123.50, 127.63, 127.839, 128.77, 128.96, 129.35, 138.63, 151.34 ($C_{10}H_6$); 173.85 (COOH). UV−vis [λ_{max}, nm (ϵ, M^{-1} cm^{-1}), phosphate buffer pH 7]: 3295 (4.33×10^3). MALDI-TOF MS: 479.926 (M^+, calcd 480.53).

9 Cascade:Dansyl[1]:(3-Oxo-2-azapropylidyne):(3-Oxo-2-azapentylidyne):Propanoic (2). As described above, dansyl chloride (0.266 g, 0.99 mmol) was stirred with the second generation amine building block (1.00 g, 0.69 mmol) in dry acetonitrile over K_2CO_3 anhydrous (0.26 g, 1.9 mmol) under N_2. After filtration and removal of the solvent, the residue was purified by column chromatography, eluting with CH_2Cl_2, followed by 5:1 CH_2Cl_2/EtOAc and finally 2:1 CH_2Cl_2/EtOAc. The recovered product (0.530 g, 46%), a pale green foam, was hydrolyzed as described above to procure a pale yellow powder in 95% yield after complete removal of the formic acid. FT-IR (KBr): 3300−2500 (ν(OH)) cm^{-1}; 3348 (ν(NH)) cm^{-1}; 1715 (ν(C═O)) cm^{-1}; 1643 (ν(AMIDE I, C═O)) cm^{-1}; 1549 (ν(AMIDE II, N−H)) cm^{-1}; 1300 (ν(C═O)) cm^{-1}; 1208 (ν(H−O)) cm^{-1}. ^{1}H NMR (DMSO-d_6): 1.62−1.92 (m, CH_2CH_2, 12H) gen 1; 1.82−2.12 (m, CH_2CH_2, 36H) gen 2; 2.86 (s, CH_3, 6H); 7.11 (sb, NH, 3H) gen 2; 7.73 (sb, NH, 1H) gen 1; 7.2−8.4 (m, $C_{10}H_6$, 6H); 12.2 (bs, OH, 9H). ^{13}C NMR (DMSO-d_6): 28.16, 29.13 (CH_2CH_2) gen 2; 30.32, 32.42 (CH_2CH_2) gen 1; 45.03 (CH_3); 56.22 ($C(CH_2CH_2)_3$) gen 2; 60.95 ($C(CH_2CH_2)_3$) gen 1; 114.81, 119.40, 123.46, 127.30, 127.68, 128.84, 128.03, 129.13, 139.43, 151.31 ($C_{10}H_6$); 171.71 (CONH); 174.53 (COOH). UV−vis [λ_{max}, nm (ϵ, M^{-1} cm^{-1}), phosphate buffer pH 7]: 329 (3.80×10^3). MALDI-TOF MS: 1168.02 (M^+, calcd 1168.23); 920.311 ($M - H_3N^+C(CH_2CH_2COOH)_3$).

(27 Cascade:Dansyl[1]:(3-Oxo-2-azapropylidyne):(3-Oxo-2-azapentylidyne):(3-Oxo-2-azapentylidyne):Propanoic (3). Following the procedure described above, dansyl chloride (0.033 g, 0.12 mmol) and the third generation amine building block (0.50 g, 0.11 mmol) were stirred in a suspension of K_2CO_3 anhydrous in dry CH_3CN under N_2. The residue obtained after filtration and solvent evaporation was purified by column chromatography (SiO_2, 5:1 CH_2Cl_2/EtOAc followed by EtOAC). A very pale green, almost white foam was recovered (0.263 g, 50%), which upon hydrolysis gave a white-green powder (95%). FT-IR (KBr): 3300−2500 (ν(OH)) cm^{-1}; 3339 (ν(NH)) cm^{-1}; 1717 (ν(C═O)) cm^{-1}; 1652 (ν(AMIDE I, C═O)) cm^{-1}; 1542 (ν(AMIDE II, N−H)) cm^{-1}; 1291 (ν(C═O)) cm^{-1}; 1203 (ν(O−H)) cm^{-1}. ^{1}H NMR (DMSO-d_6): 1.7−2.2 (m, CH_2CH_2, 156H) gen 1, 2, and 3; 2.80 (s, CH_3, 6H); 7.24 (sb, NH, 9H) gen 3; 6.9−8.5 (m, $C_{10}H_6$, 6H & NH gen1 and 2, 4H); 12.1 (bs, OH, 27H). ^{13}C NMR (DMSO-d_6): 28.10, 29.07 (CH_2CH_2) gen 3; 30.26, 30.90 (CH_2CH_2) gen 2; 44.99 (CH_3); 56.31 ($C(CH_2CH_2)_3$) gen 3; 172.26 (CONH) gen 3; 174.48 (COOH). UV−vis [λ_{max}, nm (ϵ, M^{-1} cm^{-1}), phosphate buffer pH 7]: 324 (3.31×10^3). MALDI-TOF MS: 3230.69 (M^+, calcd 3231.33); 2993.08 (M − DansylH$^+$).

3 Cascade:Nitro[1]:(3-Oxo-2-azapropylidyne):Propanoic (4). The nitrotriester (4.55 g, 10.2 mmol), precursor of Behera's amine, was hydrolyzed by stirring it in 10 mL of 96% formic acid for 15 h at 23 °C. After complete removal of the formic acid at reduced pressure and 100 °C, a white powder was obtained (2.75 g, 97%). FT-IR (KBr): 3300−2500 (ν(OH)) cm^{-1}; 1715 (ν(C═O)) cm^{-1}; 1532 (ν(N═O)) cm^{-1}; 1295 (ν(C═O)) cm^{-1}. ^{1}H NMR (DMSO-d_6): 2.1−2.2 (m, CH_2CH_2, 12H); 12.3 (bs, OH, 3H). ^{13}C NMR (DMSO-d_6): 28.16, 29.73 (CH_2CH_2); 92.77 (O_2NC); 173.04 (COOH). FAB$^+$ MS: 277 (M^+, calcd 277.23); 278 ($M + 1$).

9 Cascade:Nitro[1]:(3-Oxo-2-azapropylidyne):(3-Oxo-2-azapentylidyne):Propanoic (5). The triacid made as described above (2.5 g, 9.0 mmol) was coupled to Behera's amine (11.2 g, 27.0 mmol) in the presence of DCC (5.6 g, 27.1 mmol) and HOBT (1.23 g, 9.1 mmol). The mixture was stirred in 100 mL of dry THF for 6 days at 23 °C under N_2. The product was filtered, and after evaporation of the solvent, the residue was purified by column chromatography (2:1 CH_2Cl_2/EtOAc). Hydrolysis of the obtained white foam in 96% formic acid procured a white powder in 95% yield. FT-IR (KBr): 3300−2500 (ν(OH)) cm^{-1}; 3339 (ν(N−H)) cm^{-1}; 1721 (ν(C═O)) cm^{-1}; 1657 (ν(AMIDE I, C═O)) cm^{-1}; 1539 (ν(AMIDE I, N−H)) cm^{-1}; 1295 (ν(C═O)) cm^{-1}; 1201 (ν(O−H)) cm^{-1}. ^{1}H NMR (DMSO-d_6): 2.03 (m, CH_2CH_2, 12H); 1.75−2.12 (m, CH_2CH_2, 36H); 7.30 (bs, NH, 3H); 12.0 (bs, OH, 9H). ^{13}C NMR (DMSO-d_6): 28.00, 29.04 (CH_2CH_2); 30.06, 31.10 (CH_2CH_2); 56.39 ($C(CH_2CH_2)_3$); 93.27 (O_2NC); 170.37 (CONH); 174.32 (COOH). MALDI-TOF MS: 966.137 (M^+, calcd 964.93); 989.251 ($M + Na^+$); 1005.63 ($M + K^+$); 915.921 ($M - NO_2$).

Reagents for Photophysical Studies. DA (99%, Aldrich Chemical Co.), $Na_2HPO_4 \cdot 7H_2O$ and $NaH_2PO_4 \cdot H_2O$ (J. T. Baker, Inc.), 1,4-bis-(4-methyl-5-phenyl-2-oxazolyl)benzene (Me_2POPOP, Aldrich Chemical Co.), ethanol (dehydrated, 200 proof, Pharmco), β-CD (Sigma Chemical Co.), and polyclonal anti-dansyl antibody (rabbit IgG fraction, Molecular Probes, Inc.) were used as received. All aqueous buffer solutions were prepared from doubly distilled−deionized water (Millipore) and stock solutions were refrigerated in the dark at 4 ± 2 °C.

Instrumentation. ^{1}H and ^{13}C NMR spectra were recorded on a Varian VXR-400 spectrometer; all the chemical shift (δ) values are reported in ppm. Electronic absorption spectra were obtained in either a Shimadzu model 2101 or a Milton-Roy model 1201, equipped with a temperature-controlled cell holder that was maintained at 25 °C. FAB-MS data were recorded with a VG-Trio mass spectrometer. MALDI-TOF MS spectra were recorded at the LSU Mass Spectroscopy Facility.

Fluorescence experiments were performed with an SLM-AMINCO model 48000 MHF. For all steady-state fluorescence measurements, a 450 W xenon arc lamp was used as the excitation source with single grating monochromators serving as the wavelength selection devices. The excitation and emission spectral band-passes were kept at 8 nm, and all emission spectra were background-corrected using appropriate blanks. The time-resolved fluorescence anisotropy and intensity decay kinetics were measured in the frequency domain[12−16] using the same instrument. For these particular experiments, a CW argon-ion laser (Coherent, Innova 90−6) operating at 351.1 nm was the excitation source. An interference filter (Oriel) was placed in the excitation beam path to minimize extraneous plasma tube superradiance from reaching the detection system. The sample fluorescence was monitored in the typical L-format after passing through a 420 nm long-pass filter and a Glan-Thompson calcite polarizer. The Pockels cell modulator was operated at a 5 MHz base repetition rate. Typically, data were acquired for 60 s between 5 and 200 MHz (40 total frequencies), and at least 10 discrete multifrequency data sets were acquired for each sample. For the excited-state intensity decay measurements, we used a dilute solution of Me_2POPOP dissolved in ethanol as the reference lifetime standard; its lifetime was assigned a value of 1.45 ns.[12] Magic angle polarization conditions were used for all excited-state intensity decay measurements to eliminate bias arising from fluorophore rotational reorientation. The excited-state fluorescence lifetimes and rotational reorientation times were recovered from the frequency-domain data by using a commercially available nonlinear least-squares software package (Globals Unlimited). The actual imprecision in each datum was used as a weighting factor. Unless otherwise specified, all spectroscopic measurements were carried out at 22 ± 2 °C in 0.1 M pH 7.0 phosphate buffer. For the dynamic experiments, the samples were subjected to four freeze−pump−thaw cycles to remove residual oxygen.

Acknowledgment. The authors are grateful to the NSF for the support of this research work (to A.E.K., CHE-9982014; to F.V.B., CHE-9626636). F.V.B. is also grateful for support from the DOE (DEFG0290ER14143) and ONR (N000149610501 and N0001497100773). C.M.C. acknowledges a minority predoctoral fellowship from NIH.

JA000949L